Polyhedron 42 (2012) 66–73

Contents lists available at SciVerse ScienceDirect

Polyhedron

journal homepage: www.elsevier.com/locate/poly

cis–trans Isomerism in mixed-ligand ruthenium(II) complexes containing bis(phosphine) and azoimine ligands

Mousa Al-Noaimi [a,*], Mahmoud Sunjuk [a,*], Mohammad El-khateeb [b,1], Salim F. Haddad [c], Alaa Haniyeh [a], Murad AlDamen [c]

[a] Department of Chemistry, The Hashemite University, Zarqa, Jordan
[b] Faculty of Science and Arts at Alkamil, King Abdulaziz University, Alkamil 21931, Saudi Arabia
[c] Chemistry Department, Faculty of Science, University of Jordan, Amman, Jordan

ARTICLE INFO

Article history:
Received 10 March 2012
Accepted 30 April 2012
Available online 17 May 2012

Keywords:
Ruthenium
Complexes
Azomethine
Diphosphine ligands
X-ray structures
Electrochemistry

ABSTRACT

This study presents the syntheses and characterization of mixed-ligand azoimine-diphosphine ruthenium complexes of the general formula $[RuCl_2(Azo)(P–P)]$ (**C1**–**C5**) {Azo = $C_6H_5N{=}NC(COCH_3){=}NC_6H_5$; P–P = 1,2-bis(dimethylphosphino)ethane (dmpe) (**C1**), *cis*-1,2-bis(diphenylphosphino)ethylene (depe) (**C2**), 1.1′-bis(diphenylphosphino)methane (dppm) (**C3**), 1,2-bis(diphenylphosphino)benzene (dbpe) (**C4**),1,2-bis(di(pentaflurophenyl)phosphino)ethane (F-dppe) (**C5**)}. These complexes were synthesized via the reaction of $RuCl_3$, azoimine and the diphosphine ligands in ethanol solutions. The X-ray structure of **C2** reveals a *cis*-dichloro geometry, in spite of the bulky P–P ligand, and this is attributed to the presence of an intramolecular π–π interaction between benzene rings (on the Azo and P–P ligands) [centroid–centroid distances = 3.596 and 3.654 Å; dihedral angle between ring planes = 13.2(3) and 15.4(4)° for the two independent molecules]. In contrast, the X-ray structure of **C1**, with a less bulky dmpe ligand in which no Ph rings are available for π–π bonding, revealed a *trans*-dichloro geometry. In addition to the X-ray structures of **C1** and **C2**, this work presents and discusses the spectroscopic (IR, UV–Vis, ^{1}H NMR and ^{31}P NMR) and electrochemical (cyclic voltammetry) behavior of **C1–C5**.

1. Introduction

Metal complexes containing phosphine ligands have important industrial applications [1]. The ability of bis(dialkylphosphino)alkane ligands to donate or accept electrons from a metal center can be easily tuned by changing the alkyl groups bonded to the phosphorus atoms [1–6]. This change affects the activity, basicity, selectivity and stability of catalytic processes via ligand electronic and/or steric properties [1,5–8]. Tolman made a practical and useful separation between the electronic and the steric effects of these ligands and he was able to measure these effects [2].

Mixed-ligand diamine-bis(diphosphine) ruthenium(II) complexes have received much attention in recent years due to their remarkable performance in selective [9–11] and asymmetric [12–14] hydrogenation of unsaturated carbonyl compounds. Previously, we synthesized a family of complexes of the general type *cis*-$[Ru^{II}(dppe)LCl_2]$ {L = $C_6H_5N{=}NC(COCH_3){=}NAr$, dppe = $Ph_2P(CH_2)_2PPh_2$} [15,16] to study the effect of the substituents of the aromatic ring (Ar) on the electronic properties of the ruthenium center. The tuning of the electronic properties of the ruthenium center was monitored by the change in the energy of the MLCT bands and the redox properties. Herein, we describe the synthesis of mixed-ligand azoimine-bis(dialkylphosphine) ruthenium(II) complexes of the general formula $[RuCl_2(Azo)(P–P)]$ (**C1**–**C5**) {Azo = $C_6H_5N{=}NC(COCH_3){=}NC_6H_5$, P–P = 1,2-bis(dimethylphosphino)ethane (dmpe) (**C1**), *cis*-1,2-bis(diphenylphosphino)ethylene (depe) (**C2**), 1.1′-bis(diphenylphosphino)methane (dppm) (**C3**), 1,2-bis(diphenylphosphino)benzene (dbpe) (**C4**), 1,2-bis(di(pentaflurophenyl)phosphino)ethane (F-dppe) (**C5**)}. In addition, this work presents and discusses the spectroscopic (IR, UV–Vis, ^{1}H NMR and ^{31}P NMR) and electrochemical behavior of these complexes. The X-ray structures of complexes **C1** and **C2** are presented.

2. Experimental

2.1. Materials

The reagents, ruthenium trichloride hydrate, 1,2-bis(dimethylphosphino)ethane (dmpe), *cis*-1,2-bis(diphenylphosphino) ethylene (depe), 1.1′-bis(diphenylphosphino)methane (dppm), 1,2-bis(diphenylphosphino)benzene (dbpe), 1,2-bis(di(pentaflurophenyl)phosphino)ethane (F-dppe) and tetrabutylammonium

* Corresponding authors. Tel.: +962 5 390 3333x4315; fax: +962 5 390 3349.
E-mail addresses: manoaimi@hu.edu.jo (M. Al-Noaimi), mahmoud.sunjuk@hu.edu.jo (M. Sunjuk).
[1] Permanent address: Chemistry Department, Faculty of Science and Arts, Jordan University of Science and Technology, Irbid 22110, Jordan.

0277-5387/$ - see front matter © 2012 Elsevier Ltd. All rights reserved.
http://dx.doi.org/10.1016/j.poly.2012.04.044

hexafluorophosphate (TBAH), and the solvents (reagent grade) were purchased from Aldrich and were used as received. The synthesis and the physical characterization of the azoimine ligand (Azo) have been described previously [17].

2.2. Preparation of [$RuCl_2$(Azo)(P–P)] (**C1–C5**); general procedure

Ruthenium trichloride trihydrate (0.26 g, 1.0 mmol) and azoimine (Azo) (0.25 g, 1.0 mmol) were dissolved in 100 mL of absolute ethanol under argon. After refluxing for 1 h, 1.0 mmol of the bis(diphosphino) ligand (P–P) was added to the solution. The reaction was heated for an additional 3 h, then the solvent was removed by a rotary evaporator. The crude product was dissolved in dichloromethane and purified by chromatography (50 × 3 cm) on silica gel. The first pale yellow band of the azoimine ligand (Azo) was eluted with dichloromethane. A mixture of acetone/dichloromethane (1:1) was used to elute the second dark-red band of the product. Complexes **C1** and **C2** were recrystallized easily as dark red platelets from slowly evaporating solutions of dichloromethane.

2.3. Trans-[$RuCl_2$(Azo)(dmpe)] (**C1**)

Yield 257 mg, 45%. *Anal.* Calc. for $RuCl_2C_{21}H_{29}N_3P_2O$: C, 43.99; H, 5.10; N, 7.33. Found: C, 44.12; H, 5.30; N, 7.36%. UV–Vis in acetonitrile: λ_{max}/nm (ε_{max}/M^{-1} cm^{-1}): 326 (8.05×10^3), 375 (5.14×10^3) 547 (5.68×10^3). IR/cm^{-1}: ν(N=N) 1488, ν(C=N) 1618, ν(C=O) 1702. ^{31}P NMR ($CDCl_3$, δ ppm): 43.04 (d), 47.15 (d). ^{1}H NMR (DMSO, δ ppm): 7.14 (d, 2H, H3), 7.38 (m, 3H, H2, H1), 7.58 (m, 5H, H4, H5, H6), 2.56 (s, $COCH_3$), 1.52 (m, 4H, dmpe), 0.90 (d, 6H, dmpe), 0.82 (d, 6H, dmpe).

2.4. cis-[$RuCl_2$(Azo)(depe)] (**C2**)

Yield 286 mg, 35%. *Anal.* Calc. for $RuCl_2C_{41}H_{35}N_3P_2O$: C, 57.22; H, 4.27; N, 4.94. Found: C, 57.30; H, 4.34; N, 5.14%. UV–Vis in acetonitrile: λ_{max}/nm (ε_{max}/M^{-1} cm^{-1}): 315 (14.69×10^3), 385 (6.92×10^3), 506 (6.50×10^3). IR/cm^{-1}: ν(N=N) 1475, ν(C=N) 1623, ν(C=O) 1701. ^{31}P NMR ($CDCl_3$, δ ppm): 74.70 (d), 76.45 (d). ^{1}H NMR (DMSO, δ ppm): 2.64 (s, $COCH_3$), 6.49 (t, 2H, H5), 6.69 (d, 2H, H4), 6.83 (t, 1H, H1), 6.93 (m, 5H, depe), 7.15 (m, 15 H, depe), 7.47 (m, 3H, H3, H6), 7.56 (t, 2H, depe), 7.71 (d, 2H, H2).

2.5. cis-[$RuCl_2$(Azo)(dppm)] (**C3**)

Yield 340 mg, 40%. *Anal.* Calc. for $RuCl_2C_{40}H_{35}N_3P_2O{\cdot}0.5\ CH_2Cl_2$: C, 59.49; H, 4.37; N, 5.20. Found: C, 59.30; H, 4.77; N, 5.23%. UV–Vis in acetoinitrile: λ_{max}/nm (ε_{max}/M^{-1} cm^{-1}): 307 (8.15×10^3), 385 (7.16×10^3), 508 (6.99×10^3). IR/cm^{-1}: ν(N=N) 1486, ν(C=N) 1624, ν(C=O) 1712. ^{31}P NMR ($CDCl_3$, δ ppm): 4.75 (d), 8.43 (d). ^{1}H NMR (DMSO, δ ppm): 2.58 (s, $COCH_3$), 4.45 (d, 2H, dppm), 6.48 (t, 2H, H5), 6.69 (t, 2H, H2), 6.85 (m, 5H, dppm), 7.05 (m, 5H, dppm), 7.12 (m, 4H, H3, H4), 7.29 (t, 1H, H1), (7.33 (m,5H, dppm), 7.58 (m, 5H, dppm), 7.96 (t, 1H, H1).

2.6. cis-[$RuCl_2$(Azo)(dbpe)] (**C4**)

Yield 304 mg, 35%. *Anal.* Calc. for $RuCl_2C_{45}H_{37}N_3P_2O$: C, 62.15; H, 4.29; N, 4.83. Found: C, 62.23; H, 4.07; N, 4.53%. UV–Vis in acetonitrile: λ_{max}/nm (ε_{max}/M^{-1} cm^{-1}): 306 (6.42×10^3), 368 (6.64×10^3), 509 (6.71×10^3). IR/cm^{-1}: ν(N=N) 1486, ν(C=N) 1619, ν(C=O) 1711. ^{31}P NMR ($CDCl_3$, δ ppm): 69.70 (d), 75.69 (d). ^{1}H NMR (DMSO, δ ppm): 2.26 (s, $COCH_3$), 6.49 (m, 4H, dbpe), 6.72 (d, 2H, H4), 4.86 (m, 5H, dbpe), 6.95 (m, 3H, H5, H6), 7.01 (t, 2H, H2), 7.15 (d, 2H, H4), 7.26 (m, 3H, dbpe), 7.02(t, 1H, H1), 7.35 (m, 6H, dbpe), 7.45 (m, 3H, dbpe), 7.62 (m, 3H, dbpe).

2.7. cis-[$RuCl_2$(Azo)(F-dppe)] (**C5**)

Yield 235 mg, 20%. *Anal.* Calc. for $RuCl_2C_{41}H_{13}N_3P_2F_{20}O$: C, 41.82; H, 1.11; N, 3.57. Found: C, 41.64; H, 1.07; N, 3.83%. UV–Vis in acetonitrile: λ_{max}/nm (ε_{max}/M^{-1} cm^{-1}): 340 (8.78×10^3), 396 (8.87×10^3), 513 (6.20×10^3). IR/cm^{-1}: ν(N=N) 1478, ν(C=N) 1612, ν(C=O) 1709. ^{31}P NMR ($CDCl_3$, δ ppm): 95.41 (d), 106.81 (d). ^{1}H NMR (DMSO, δ ppm): 2.26 (s, $COCH_3$), 1.75 (m, 4H, F-dppe), 7.11 (d, 2H, H4), 7.21 (t, 2H, H5), 7.28 (t, 1H, H6), 7.35 (t, 2H, H2), 7.45 (t, 1H, H1), 7.54 (d, 2H, H3).

2.8. Instrumentation

Electrochemical measurements were performed in acetonitrile (Aldrich, HPLC grade) using a Volta Lab model PGP201 with a platinum disk working electrode (1.6-mm diameter), a platinum wire counter electrode and a silver wire pseudo-reference electrode. Ferrocene (0.665 V versus NHE) was used as an internal reference [18]. The temperature was controlled (at 25.0 ± 0.1 °C) by a Haake D8-G refrigerator. Tetrabutylammonium hexafluorophosphate (0.10 M) was twice recrystallized and vacuum dried at 120 °C, and used as the supporting electrolyte. IR spectra were measured on a FT-IR JASCO model 420 spectrophotometer. Nuclear magnetic resonances (^{1}H and ^{31}P NMR) spectra were measured on a Bruker-Avance 400 MHz spectrometer at 400 and 161.3 MHz, respectively. All chemical shifts are reported in ppm downfield of TMS (^{1}H) or 85% phosphoric acid (^{31}P) and referenced using the chemical shifts of residual solvent resonances. Elemental analyses were carried out on a Euro vector E.A.3000 instrument using copper sample-tubes.

2.9. X-ray crystallography

Suitable crystals of complexes **C1** and **C2** were selected and attached to oil dipped fibers. The data were collected at 100(1) K for **C1** using a Gemini E Ultra/Oxford Diffractometer equipped with an E O S CCD detector and a Cryojet XL low temperature device, and at 291(2) K for **C2** using an Oxford Diffraction Xcaliburs. For **C1** and **C2**, CrysAlisPro software [19] was used for data collection and reduction. Both structures were solved by direct methods, using the program OLEX2 [20], followed by Fourier synthesis, and refined on F^2 with SHELXL-97 [21]. The hydrogen atoms were positioned constrained and assigned isotropic thermal parameters of 1.2 times the riding atoms. A summary of the crystallographic data and structure refinement parameters for **C1** and **C2** is given in Table 1.

The **C2** structure was solved in the $P\bar{1}$ space group. There are four molecular units, $C_{41}H_{35}Cl_2N_3OP_2Ru$, in the cell, with two molecules per asymmetric unit. There was also a region around the center of inversion with residual peaks that seemed to be due to disordered water molecules. Molecule analysis by the program PLATON [22] using the squeeze routine indicated a void space of 210 Å^3. On squeezing out this disordered region, the refinement converged at R_1 = 0.0631, S = 1.080 and the largest electron density peak of 0.401 Å^3 was located 0.627 Å^3 off Ru1. No decomposition was observed during data collection. Anisotropic least-squares refinement of non-H atoms was applied. The crystal structure of the complex **C2** is depicted in Fig. 2. Crystal data after void squeeze is given in Table 1 and selected bond distances and angles are given in Table 3.

The **C1** structure was solved in the $P1211$ space group. There are two molecular units, $C_{21}H_{29}Cl_2N_2OP_2Ru$, in the asymmetric unit. The crystal was found to be a pseudo-merohedral twin. Twin law 2-fold rotation about the *a*-axis (or equivalently about the *c*-axis) was applied. The volume fraction of the twin domains is approximately in the ratio 72:28. The diffraction images show some spots to be badly split. The mosaic spot spread was very

Table 1
Crystal data and structure refinement for complexes **C1** and **C2**.

Complex	**C1**	**C2**
Empirical formula	$C_{21}H_{29}Cl_2N_3OP_2Ru$	$C_{41}H_{35}Cl_2N_3OP_2Ru$
Formula weight	573.38	819.63
Temperature (K)	100.0	291
Wavelength (Å)	0.7107	0.7107
Crystal system	monoclinic	triclinic
Space group	$P1211$	$P\bar{1}$
Unit cell dimensions		
a (Å)	9.9695(6)	11.8545(5)
b (Å)	22.2516(13)	14.7083(5)
c (Å)	10.8470(6)	23.9846(8)
Volume (Å^3)	2406.2(2)	3993.7(3)
Z	4	4
Density (calculated) (Mg/m^3)	1.583	1.363
Absorption coefficient (mm^{-1})	1.025	0.641
$F(000)$	1168	1672
Crystal size (mm^3)	0.30 × 0.27 × 0.19	0.35 × 0.23 × 0.15
Theta range for data collection (°)	3.76–25.03	2.88–25.03
Index ranges	$-11 \leqslant h \leqslant 11$ $-26 \leqslant k \leqslant 26$ $-12 \leqslant l \leqslant 12$	$-14 \leqslant h \leqslant 13$ $-17 \leqslant k \leqslant 17$ $-28 \leqslant l \leqslant 25$
Reflections collected	24225	35447
Independent reflections	8448 [R_{int} = 0.0587]	14089 [R_{int} = 0.0435]
Completeness to theta = 25.03°	99.6%	99.8%
Maximum and minimum transmission	0.8259 and 0.7498	0.401 and 0.627
Refinement method	full-matrix least-squares on F^2	full-matrix least-squares on F^2
Data/restraints/parameters	8448/1/302	14089/0/902
Goodness-of-fit on F^2	1.116	1.080
Final R indices [$I > 2\sigma(I)$]	R_1 = 0.0965, wR_2 = 0.2350	R_1 = 0.0631, wR_2 = 0.1228
R indices (all data)	R_1 = 0.1014, wR_2 = 0.2380	R_1 = 0.0909, wR_2 = 0.1332
Largest difference in peak and hole (e Å^{-3})	2.318 and −1.942	0.78 and −0.84

$R_1 = \Sigma||F_o| - |F_c||/\Sigma|F_o|$; $wR_2 = \{\Sigma[w(F_o^2 - F_c^2)^2]/\Sigma[w(F_o^2)^2]\}^{1/2}$.

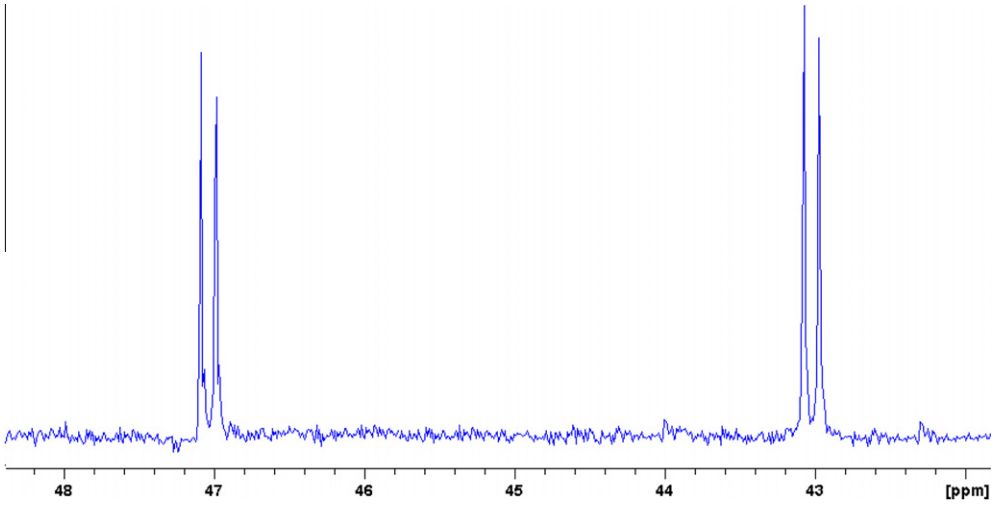

Fig. 1. $^{31}P\{^1H\}$ NMR (300 MHz, $CDCl_3$, 25 °C) spectra for complex **C1**.

wide, so the scan width was dropped to 0.5 degrees; even so, there were about 18% of overlapped pixels. The R_1 value dropped from about 0.18 to about 0.10, S = 1.116 when the second (merohedral) twin component was introduced into the refinement. The data quality did not allow anisotropic refinement for all non-hydrogen atoms. The crystal structure of the complex **C1** is depicted in Fig. 1 and selected bond distances and angles are given in Table 2.

3. Results and discussion

3.1. Synthesis

A previous study showed that the products of the reaction of the bulky diphosphine ligand dppe with substituted azoimine ligands (Azo) and $RuCl_3$ are *cis*-[$RuCl_2$(Azo)(dppe)] complexes [15]. The

Table 2
Selected bond lengths (Å) and angles (°) for complex **C1**.

Complex **C1**			
Molecule (1)		Molecule (2)	
Bond lengths (Å)			
Ru(1)–N(1)	2.08(2)	Ru(31)–N(31)	1.990(14)
Ru(1)–N(3)	2.101(14)	Ru(31)–N(33)	2.051(11)
Ru(1)–P(1)	2.348(6)	Ru(31)–P(31)	2.363(5)
Ru(1)–Cl(1)	2.364(6)	Ru(31)–Cl(31)	2.364(6)
Ru(1)–P(2)	2.378(5)	Ru(31)–Cl(32)	2.364(5)
Ru(1)–Cl(2)	2.378(6)	Ru(31)–P(32)	2.392(5)
N(1)–N(2)	1.22(2)	N(31)–N(32)	1.30(2)
N(2)–C(7)	1.40(2)	N(31)–C(31)	1.45(2)
N(3)–C(7)	1.18(2)	N(32)–C(37)	1.44(2)
Bond angles (°)			
N(1)–Ru(1)–N(3)	71.1(7)	N(31)–Ru(31)–N(33)	74.5(5)
N(1)–Ru(1)–P(1)	101.7(6)	N(31)–Ru(31)–P(31)	100.5(4)
N(3)–Ru(1)–P(1)	172.8(4)	N(33)–Ru(31)–P(31)	174.8(4)
N(1)–Ru(1)–Cl(1)	97.5(6)	N(31)–Ru(31)–Cl(31)	93.0(4)
N(3)–Ru(1)–Cl(1)	93.2(4)	N(33)–Ru(31)–Cl(31)	93.3(4)
P(1)–Ru(1)–Cl(1)	88.6(2)	P(31)–Ru(31)–Cl(31)	85.45(19)
N(1)–Ru(1)–P(2)	175.2(6)	N(31)–Ru(31)–Cl(32)	93.9(4)
N(3)–Ru(1)–P(2)	104.4(4)	N(33)–Ru(31)–Cl(32)	92.8(4)
P(1)–Ru(1)–P(2)	82.75(17)	P(31)–Ru(31)–Cl(32)	89.0(2)
Cl(1)–Ru(1)–P(2)	84.3(2)	Cl(31)–Ru(31)–Cl(32)	171.8(2)
N(1)–Ru(1)–Cl(2)	91.1(6)	N(31)–Ru(31)–P(32)	175.9(4)
N(3)–Ru(1)–Cl(2)	93.2(4)	N(33)–Ru(31)–P(32)	101.5(3)
P(1)–Ru(1)–Cl(2)	85.8(2)	P(31)–Ru(31)–P(32)	83.51(18)
Cl(1)–Ru(1)–Cl(2)	170.6(2)	Cl(31)–Ru(31)–P(32)	87.9(2)
P(2)–Ru(1)–Cl(2)	87.5(2)	Cl(32)–Ru(31)–P(32)	85.6(2)

formation of the thermodynamically stable products (*cis*-isomer) was supported by an X-ray structure determination [15,16]. Herein, the sequential addition of equimolar amounts of azoimine (Azo), different bis(diphosphine) ligands (P–P) and $RuCl_3$ in ethanol as the solvent gives the air-stable *trans*-[$RuCl_2$(dmpe)(Azo)] (**C1**) and *cis*-[$RuCl_2$(P-P)(Azo)] (**C2–C5**) (Scheme 1). Although both *cis* and *trans* isomers of [$RuCl_2$(Azo)(P–P)] (**C1–C5**) could be excepted as products of these syntheses, purification by silica gel showed only one product. The isolated products are expected to be of a *trans*-geometry for **C1** and *cis*-geometry for **C2–C5**, as proved by X-ray crystal structure determination. Complexes **C1–C5** have been characterized by elemental analysis, infrared spectroscopy, ^{1}H and ^{31}P{^{1}H} NMR spectroscopy, as well as X-ray structure determination for complexes **C1** and **C2**.

The IR spectra of the complexes **C1–C5** show three sets of characteristic absorptions in the ranges 1701–1712, 1618–1624 and 1475–1488 cm^{-1}, which can be assigned to C=O of the acetyl group, C=N and N=N double bonds, respectively.

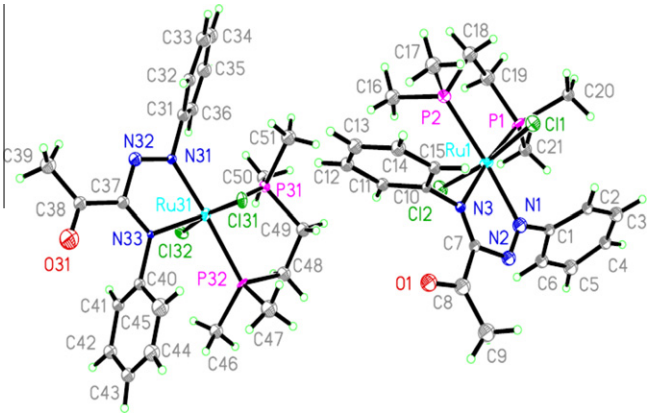

Fig. 2. Thermal ellipsoid drawing (30%) of complex **C1** showing the two independent molecules of the Ru complex.

The ^{1}H NMR spectrum of **C1** shows a multiplet at 1.52 ppm which is assigned to the four protons of the two CH_2 groups of the dmpe ligand. The two doublets at 0.82 and 0.90 ppm are assigned to the 12 protons of the 4-methyl groups of the dmpe ligand, while the protons of the acetyl group of the Azo ligand appear as a singlet at 2.56 ppm. The aromatic region in the ^{1}H NMR spectra of complexes **C2–C5** consists of several coupled multiplets due to the aromatic protons of the phenyl rings of the diphosphine and the azoimine ligands.

The ^{31}P{^{1}H} NMR spectrum of *trans*-[$RuCl_2$(dmpe)(Azo)] (**C1**) (Fig. 1) shows two doublets which are assigned to the two types of phosphorus atoms, indicating an AMX spin system. These doublets appeared as broad bands at 43.04 and 47.15 ppm due to the coupling of the two phosphorus atoms of the P–P ligand. It is suggested that the shielded signal refers to the phosphorus atom *trans* to the imine nitrogen of the azoimine ligand and the deshielded signal refers to the phosphorus atom *trans* to the azo nitrogen atom [23]. Moreover, complexes **C2–C5** have magnetic non-equivalent phosphorus atoms (P *trans* to Cl and P *trans* to the nitrogen of the Azo ligand), which appear as two doublets. It is also suggested that the shielded signal refers to the phosphorous *trans* to the nitrogen of the azoimine and the deshielded signal refers to the phosphorous atom *trans* to the Cl atom [23], which is consistent with a structure in which the chlorides are mutually in *cis*-positions. It is well known that the P–P chelates possess three major characteristics: electron-donating ability, steric properties and a rigid P–M–P angle, often called the "bite angle" [8,24]. For the four-membered chelate complex **C3**, the phosphorus resonates at the

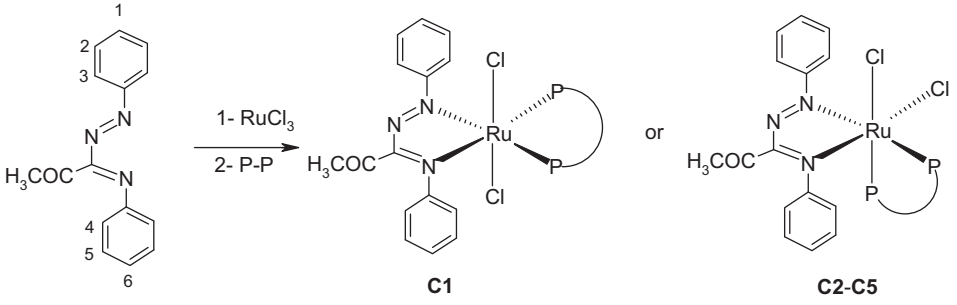

P-P ligand	dmpe	depe	dppm	dbpe	F-dppe
Complex	**C1**	**C2**	**C3**	**C4**	**C5**

Scheme 1. The chemical structures of the ligand (Azo) and the complexes **C1–C5**.

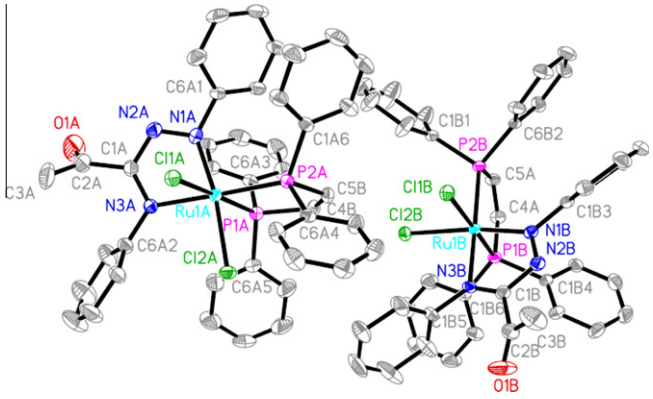

Fig. 3. Thermal ellipsoid drawing (30%) of complex **C2** showing the two independent molecules of the Ru complex.

highest field, whereas the resonances of the five-membered ring containing complexes **C1**, **C2**, **C4** and **C5** are observed at lower fields [25]. For the five-membered chelates **C1**, **C2**, **C4** and **C5**, the **C1** resonance is found at the lowest field. The difference in the chemical shift can be explained by the C–P–C bond angle [24]; as the cone angle increases, the phosphorus chemical shift moves upfield. The effect of the double bond between the two P–P atoms on the electronic delocalization makes the phosphorus atoms more deshielded and the peaks appear at 74.70 and 76.45 ppm for **C2** and at 69.70 and 75.69 ppm for **C4**. A similar effect has been observed in the series $[Pd(S_2CNEt_2)(P–P)]^+$ [26], *trans*-$[RuCl_2(P–P)_2]$ [27] and *fac*-$[RuCl_3(NO)(P–P)]$ [28]. Increasing the electron withdrawing ability of the substituent on the phenyl ring (as in **C5**) decreases the electron density on the phosphorus atom and thus shifts the $^{31}P\{^1H\}$ NMR peaks to higher values, 95.41 and 106.81 ppm compared to *cis*-$[RuCl_2(Azo)(dppe)]$ [15].

Table 3
Selected bond lengths (Å) and angles (°) for complex **C2**.

Complex **C2**			
Molecule (A)		Molecule (B)	
Bond lengths (Å)			
Ru(1A)–N(1A)	1.967(4)	Ru(1B)–N(1B)	1.971(4).
Ru(1A)–N(3A)	2.117(4)	Ru(1B)–N(3B)	2.105(4)
Ru(1A)–P(1A)	2.3273(14)	Ru(1B)–P(1B)	2.3208(15)
Ru(1A)–P(2A)	2.3465(14)	Ru(1B)–P(2B)	2.3454(14)
Ru(1A)–Cl(2A)	2.4018(14)	Ru(1B)–Cl(2B)	2.3809(15)
Ru(1A)–Cl(1A)	2.4414(14)	Ru(1B)–Cl(1B)	2.4393(14)
N(1A)–N(2A)	1.314(6)	N(2B)–N(1B)	1.321(6)
N(3A)–C(1A)	1.312(7)	N(3B)–C(1B)	1.293(7)
N(2A)–C(1A)	1.357(7)	N(2B)–N(1B)	1.359(7)
Bond angles (°)			
N(1A)–Ru(1A)–N(3A)	76.62(18)	N(1B)–Ru(1B)–N(3B)	76.39(18)
N(1A)–Ru(1A)–P(1A)	99.20(13)	N(1B)–Ru(1B)–P(1B)	99.39(12)
N(3A)–Ru(1A)–P(1A)	100.15(12)	N(3B)–Ru(1B)–P(1B)	98.34(12)
N(1A)–Ru(1A)–P(2A)	102.99(14)	N(1B)–Ru(1B)–P(2B)	103.33(13)
N(3A)–Ru(1A)–P(2A)	176.33(12)	N(3B)–Ru(1B)–P(2B)	178.02(13)
P(1A)–Ru(1A)–P(2A)	83.53(5)	P(1B)–Ru(1B)–P(2B)	83.64(5)
N(1A)–Ru(1A)–Cl(2A)	171.27(14)	N(1B)–Ru(1B)–Cl(2B)	169.55(13)
N(3A)–Ru(1A)–Cl(2A)	94.88(13)	N(3B)–Ru(1B)–Cl(2B)	93.88(13)
P(1A)–Ru(1A)–Cl(2A)	84.14(5)	P(1B)–Ru(1B)–Cl(2B)	85.68(5)
P(2A)–Ru(1A)–Cl(2A)	85.35(5)	P(2B)–Ru(1B)–Cl(2B)	86.25(5)
N(1A)–Ru(1A)–Cl(1A)	84.98(13)	N(1B)–Ru(1B)–Cl(1B)	84.70(12)
N(3A)–Ru(1A)–Cl(1A)	83.40(12)	N(3B)–Ru(1B)–Cl(1B)	85.05(12)
P(1A)–Ru(1A)–Cl(1A)	175.02(5)	P(1B)–Ru(1B)–Cl(1B)	175.19(5)
P(2A)–Ru(1A)–Cl(1A)	92.92(5)	P(2B)–Ru(1B)–Cl(1B)	92.97(5)
Cl(2A)–Ru(1A)–Cl(1A)	92.11(5)	Cl(2B)–Ru(1B)–Cl(1B)	90.71(5)

3.2. Crystal structures

X-ray crystal structures of complexes **C1** and **C2** were obtained and the molecular structures are shown in Figs. 2 and 3, respectively. Selected bond lengths and angles are given in Tables 2 and 3. There are two independent but structurally similar molecules in the asymmetric unit. For complex **C1** (Fig. 2), the donor atoms around the Ru(II) center occupy *cis:cis:trans* N,N:P,P:Cl,Cl positions with average bit angles for N–Ru–N and P–Ru–P of 72.8° and 83.13°, respectively. On the other hand, for complex **C2** (Fig. 3), the donor atoms occupy *cis:cis:cis* N,N:P,P:Cl,Cl positions with average bite angles for N–Ru–N, P–Ru–P and Cl–Ru–Cl of 76.50°, 83.59° and 91.41°, respectively. These angles indicate a distorted octahedral coordination geometry in both complexes.

The azoimine (Azo) ligand in **C1** is chelating via its N1 (azo) and N3 (imine) in molecule 1 and N31 (azo) and N33 (imine) in molecule 2, thus forming five-membered chelate rings with average Ru(II)–N(azo) and Ru(II)–N(imine) distances of 2.035 and 2.076 Å, respectively. The dmpe ligand is also chelating via its two P-atoms, with an average Ru–P distance of 2.356 Å. The average Ru–P (Ru–P2 and Ru-P32) distance *trans* to Ru–N(azo) (Ru-N1 and Ru-N31) of 2.385 Å is longer than the Ru–P distance *trans* to Ru–N(imine) of 2.356 Å. The two chloride ligands are *trans* to each other with an average Ru–Cl distance of 2.368 Å. The Ru-N, Ru-P and Ru-Cl bond lengths are within the well established range of Ru(II) complexes containing these atoms [29–31]. For complex **C2** (Fig. 3), the azoimine (Azo) is chelating via its N1A (azo) and N3A (imine) in molecule A and N1B (azo) and N3B (imine) in molecule B, with average Ru(II)–N(azo) and Ru(II)–N(imine) distances of 1.969 and 2.111 Å, respectively. This observation suggests that there is a strong back donation to the azoimine ligand and this back donation is localized in the azo group [32]. However, it is interesting to note that the extent of the π-back donation is also affected by the geometry of the $[RuCl_2(Azo)(P–P)]$ complexes. For *cis*-**C2** the azo group, which is *trans* to the π-donor chloride ligand, has an average Ru–N(azo) bond length of 1.969 Å, and this is slightly shorter than the corresponding bond of *trans*-**C1** (2.035 Å). In contrast, the average N=N(azo) bond length of **C2** (1.303 Å) is similar to that in *cis*-$[RuCl_2(dppe)(Azo)]$ (**C6**) [15], but slightly longer than that in **C1** (1.260 Å). The average Ru(II)–Cl2 distance (2.392 Å) *trans* to the strong π-acceptor N(azo) is longer than Ru(II)–Cl1 (2.441 Å), *trans* to better a σ-donor and weak π-acceptor phosphorus atom.

Recently, π–π interactions have been revealed as important factors in deciding ligand arrangements and molecular structures [33]. It is important to note that a *cis* or *trans* geometry of the complexes **C1**–**C5** depends upon the presence of a π–π interaction be-

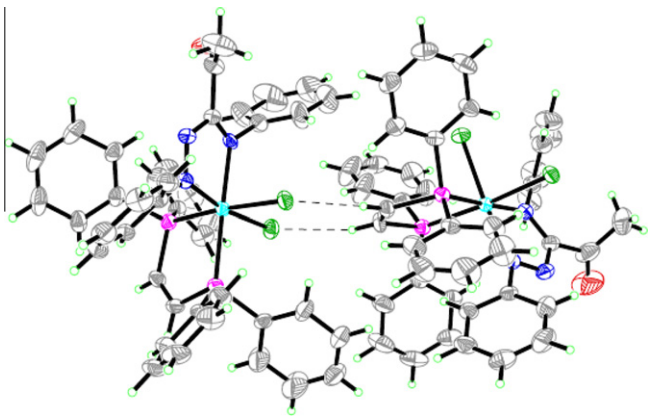

Fig. 4. A view of the crystal structure of **C2**, showing the intramolecular Cl---H–C intramolecular interactions.

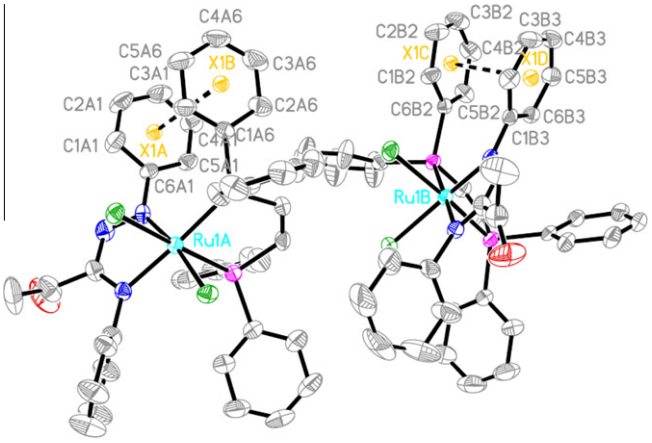

Fig. 5. A view of the crystal structure of **C2**, showing the intramolecular π–π intramolecular interaction between one phenyl ring of the bis-diphenylphosphine ligand and one phenyl ring of the azoimine ligand.

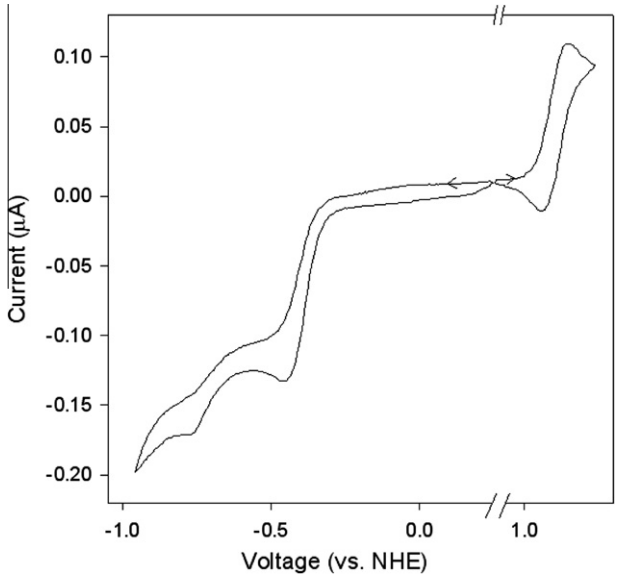

Fig. 6. Cyclic voltammogram for complex **C1** in acetonitrile 0.1 M TBAH at 25 °C, data reported in V vs. NHE with scan rate of 0.1 V/s

tween one of the phenyl rings of the bis-diphenylphosphine ligand and one of the phenyl rings of the azoimine ligand, and not on the steric hindrance (size) of the diphosphine ligands. If ligand volume was the only factor which determines the complex stereochemistry, then large diphosphine ligands would render *trans* isomers because the ligand steric interactions are minimized in this arrangement. For **C2**, There are Cl---H–C intermolecular (Fig. 4) and π–π intramolecular interactions (Fig. 5). The π–π intramolecular interaction between one phenyl ring of the bis-diphenylphosphine ligand and one phenyl ring of the azoimine ligand is possible due to the disposition and proximity of the rings. This π–π interaction is maximized in the *cis* chlorine configuration (**C2–C5**) (Fig. 4). The normal to the plane of the ring including C1A1 to C6A1 (centroid X1A) makes an angle of 13.2(3)° with the normal to the plane of the ring including C1A6 to C6A6 (centroid X1B), and the X1A...X1B separation is 3.596 Å. The normal to the plane of the ring including C1B2 to C6B2 (centroid X1C) makes an angle of 15.5(4)° with the normal to the plane of the ring including C1B3 to C6B3 (centroid X1D), and the X1C...X1D separation is 3.654 Å. Complex **C1** has a dmpe ligand (no Ph rings) and, therefore, has a *trans* structure since a π–π interaction is not possible. The crystal structure of **C2** reveals two Cl---H-C intramolecular interactions with Cl---C distances of 3.415 and 3.603 Å.

3.3. Electrochemistry

The electron-transfer behavior of the complexes in acetonitrile solution was examined by cyclic voltammetry and the corresponding results are summarized in Table 4. As a representative example, the cyclic voltammogram for complex **C1** is shown in Fig. 6. Two one-electron reduction steps are observed in the range −0.12 to −0.71 V versus NHE, and these are localized at the azo group, analogous to the azopyridine systems [31]. Our concern here is the quasi-reversible single oxidation wave which lies between 1.15 and 1.52 V. The multi scan CV of the complexes in this region indicated that these complexes are electrochemically stable. This wave is assigned to Ru(III/II) and occurs at more positive potentials compared to the analogous dihalo ruthenium(II) complexes [34]. The large anodic shift for this family (compared to the $[RuCl_2(Azo)(bpy)]$ complex [35]) results from the decrease of electron density transferred to the metal by the diphosphine (P–P) ligand [36].

On comparing the Ru(III/II) redox couple for the *trans*-complex **C1** with the *cis*-complexes **C2**-**C5**, there is a decrease in the oxidation potential by 300 mV on going from the *trans*-complex **C1** to the *cis*-complexes **C2–C4** and 100 mV on going to the *cis* complex **C5**. The decrease in Ru(III/II) redox couple for the *trans*-complex **C1** relative to *cis*-complexes (**C2**-**C5**) is well established in Ru(II) chemistry [37]. For the *trans*-complex **C1**, the competition between dmpe and the azoimine ligands for the π-electrons of the ruthenium atom makes the metal electron-rich and decreases the oxidation potential compared to the *cis*-complexes **C2**–**C5** [38].

For the series *cis*-$[RuCl_2(Azo)(P\text{-}P)]$ (**C2**–**C5**), the differences in the Ru(III/II) values are related to the stability of the diphosphine complexes. Consequently, the less stable complex is easier to oxidize. A similar behavior was observed for the $[Ru(Cp)(P–P)(NO_2)]$ series (P–P = dppe, dppm or dmpe) [36] in which the ruthenium(III/II) redox potential shifted to more anodic potentials when the more stable complex (P–P = dppe, dppm) is replaced by the less stable $[Ru(Cp)(dmpe)(NO_2)]$ complex [38]. The large decrease in the oxidation potential for the less stable complex **C5** compared to the more stable complexes **C2**–**C4** and *cis*-$[RuCl_2(Azo)(dppe)]$ [15] is due to the strong electron withdrawing fluorine atoms in the phenyl rings which reduces the basicity of the P–P ligands, and consequently the stability of **C5**.

Table 4
Cyclic voltammetry and electronic spectroscopic data of *cis*-$[RuCl_2(P\text{-}P)(Azo)]$ (**C2**–**C5**) and *cis*-$[RuCl_2(dppe)(Azo)]$ (**C6**) [15].

Complexes[a]	Ru(III/II) [b]	Azo(0/−)[c]	(Δ*E*) [d]	λ_{max} (nm) [e], energy (eV)[e]
C1	1.15	−0.45	1.60	547, 2.267
C2	1.45	−0.28	1.73	506, 2.450
C3	1.52	−0.12	1.64	508, 2.440
C4	1.49	−0.22	1.71	506, 2.450
C5	1.25	−0.17	1.42	513, 2.417
C6	1.50	−0.28	1.78	504, 2.460

[a] Solvent MeCN, supporting electrolyte Bu_4NPF_6 (0.1 M), scan rate 0.1 V s), Pt-disk working electrode, Pt-wire auxiliary electrode, reference electrode Ag at 25 °C.
[b] Ru(III/II) = (E°pa + E°pc)/2.
[c] The cathodic peak maximum.
[d] ΔE° = Ru(III/II) − Azo(0/−).
[e] MLCT = [1239.8/λ_{max}(nm)] eV.

3.4. Absorption spectra

UV–Vis electronic absorption spectra of all the complexes were measured in acetonitrile. Fig. 7 shows the electronic spectra of

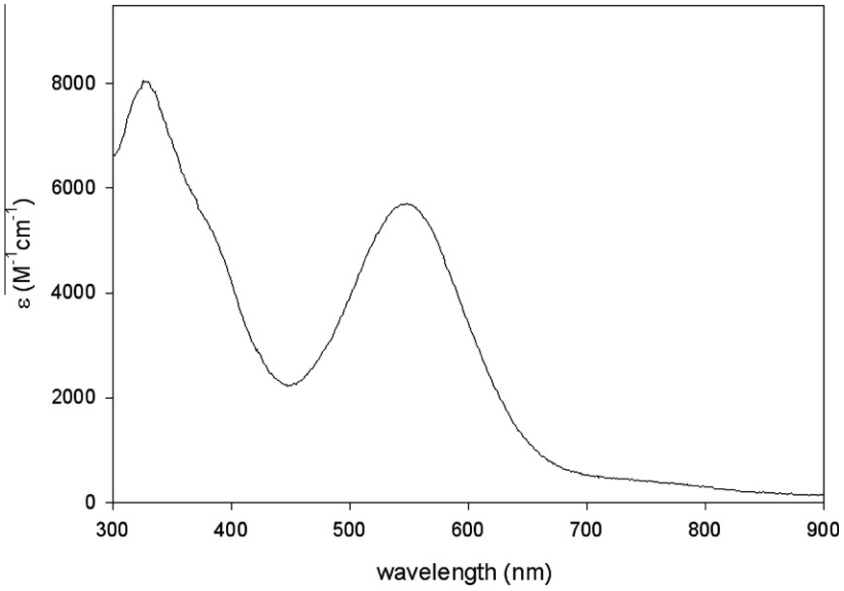

Fig. 7. UV–Vis spectrum for complex **C1** in acetonitrile.

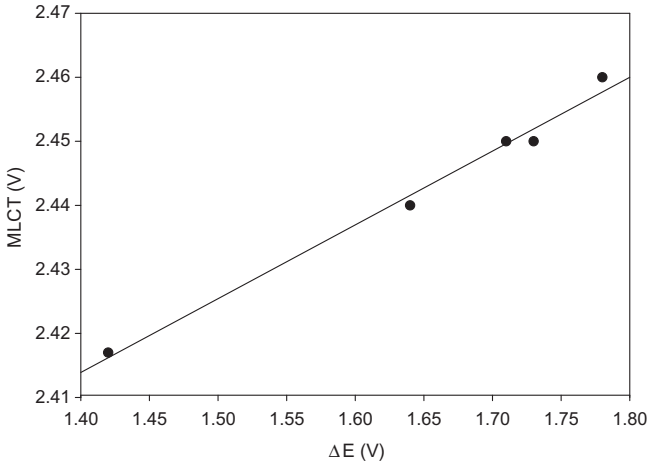

Fig. 8. Linear correlation between MLCT band energies and ΔE° for *cis*-[$RuCl_2$(P-P)(Azo)] (**C2**–**C5**) and *cis*-[$RuCl_2$(dppe)(Azo)] (**C6**) [15]. ΔE° = Ru(III/II)-Azo(0/−) in volts. The equation of the line is (E_{MLCT} = 0.11 ΔE° + 2.25).

complex **C1**, and the changes in the λ_{max} values are tabulated in Table 1, based on the change in the bis(diphosphine) ligand. Complex **C1**, as representative example, has three bands: two transitions at λ = 326 and 375 nm, which are assigned as ligand–ligand charge transfer (LLCT) type, and a transition in the visible region at 547 nm which is assigned to a MLCT transition [15,16].

The difference in the two successive redox responses at potentials positive and negative to NHE [ΔE° = Ru(III/II) − Azo(0/−)] may be correlated with the low energy MLCT [t(Ru) → π^*(azomethine)] transition [39]. Since the electronic excitation may be considered as an intramolecular redox process [40], the spin-allowed MLCT transition is expected to be linearly related to ΔE°. The least squares plot of E_{MLCT} against ΔE° among the entire group of *cis*-complexes (Fig. 8) gave a linear correlation (E_{MLCT} = 0.11 ΔE° + 2.25), however the slope of the line is only 0.11. This may result from solvent effects that account for the small changes of energy in this group of complexes [39].

4. Conclusion

This work presents a study on the dependence of the product geometry (*cis* versus *trans*) on the P–P ligand of the reaction of $RuCl_3$ and azoimine with different alkyl and aryl diphosphine (P–P) ligands. Based on the X-ray structures, the π–π intramolecular stabilizing interaction is an important factor in deciding ligand arrangements and molecular structures. This stabilizing interaction is maximized in the aryl diphosphine ligands (P–P = depe, dppm, dbpe, F-dppe) which results in *cis*-[$RuCl_2$(P-P)(Azo)] as the main product. For the alkyl bis(phosphine) ligand (P–P = dmpe), the main product is the *trans* one. There is a decrease in oxidation potential going from *cis*-[$RuCl_2$(P–P)(Azo)] (**C2**, **C3** and **C4**) to the *trans*-complex. The differences in the $E_{1/2}$ values for the *cis*-family **C2**–**C5** are related to the stability of the bis(phosphine) complexes. Consequently, the less stable complex **C5** is easier to oxidize. The chemical shifts of the $^{31}P\{^1H\}$ NMR spectra are also related to the C–P–C bond angle, electron-donating ability of the P–P chelates, the steric properties and the rigid P–M–P bite angle.

Acknowledgments

The authors would like to thank the Hashemite University (Jordan). Thanks are also extended to Dr. Christopher Ceccarelli, Applications Scientist, Agilent Technologies Inc., Blacksburg, VA 24060.

Appendix A. Supplementary material

CCDC 847801 and 859317 contain the supplementary crystallographic data for **C1** and **C2**. These data can be obtained free of charge via http://www.ccdc.cam.ac.uk/conts/retrieving.html, or from the Cambridge Crystallographic Data Centre, 12 Union Road, Cambridge CB2 1EZ, UK; fax: (+44) 1223-336-033; or e-mail: deposit@ccdc.cam.ac.uk.

References

[1] J.K. Whitesell, Chem. Rev. 89 (1989) 1581.
[2] C.A. Tolman, Chem. Rev. 77 (1977) 313.
[3] M. El-khateeb, M. Al-Noaimi, Z. Al-Amawi, A. Roller, S. Shova, Inorg. Chim. Acta 361 (2008) 2957.
[4] J.M. Brown, Chem. Soc. Rev. 22 (1993) 25.

[5] M. Sunjuk, M. Al-Noaimi, Y. Al-Degs, T. Al-Qirem, E. Lindner, A. Abu-Surrah, J. Polym. Sci., Part A 47 (2009) 6715.
[6] M. Sunjuk, M. Al-Noaimi, G. Abu Sheikha, E. Lindner, B. El-Eswed, K. Sweidan, Polyhedron 28 (2009) 1393.
[7] J.A. Cabeza, Organometallics 12 (1993) 4141.
[8] M.N. Golovin, Organometallics 4 (1985) 1981.
[9] E. Lindner, I. Warad, K. Eichele, H.A. Mayer, Inorg. Chim. Acta 350 (2003) 49.
[10] E. Lindner, A. Ghanem, I. Warad, K. Eichele, H.A. Mayer, V. Schurig, Tetrahedron: Asymmetry 14 (2003) 1045.
[11] C. Nachtigal, S. Al Gharabli, K. Eichele, E. Lindner, H.A. Mayer, Organometallics 21 (2002) 105.
[12] R. Noyori, T. Okhuma, Angew. Chem., Int. Ed. Engl. 40 (2001) 40.
[13] R. Noyori, M. Yamakawa, S. Hashiguchi, J. Org. Chem. 66 (2001) 7931.
[14] K. Abdur-Rashid, M. Faatz, A.J. Lough, R.H. Morris, J. Am. Chem. Soc. 123 (2001) 7473.
[15] M. Al-Noaimi, M. El-Barghouthi, M. El-khateeb, O. Abdel-Rahman, H. Görls, R.J. Crutchley, Polyhedron 27 (2008) 2698.
[16] M. Al-Noaimi, M.I. El-Barghouthi, O.S. Abdel-Rahman, S.F. Haddad, A. Rawashdeh, Polyhedron 30 (2011) 1884.
[17] M. Al-Noaimi, H. Saadeh, S. Haddad, M. El-Barghouthi, M. El-khateeb, R.J. Crutchley, Polyhedron 26 (2007) 3675.
[18] T. Gennett, D.F. Milner, M.J. Weaver, J. Phys. Chem. 89 (1985) 2787.
[19] Oxford Diffraction Ltd., CrysAlis Software Systems (version 1.171), Oxford, England, 2002.
[20] O.V. Dolomanov, L.J. Bourhis, R.J. Gildea, J.A.K. Howard, H. Puschmann, J. Appl. Crystallogr. 42 (2009) 339.
[21] G.M. Sheldrick, SHELXL-97, Program for X-ray Crystal Structure Refinement, University of Goettingen, Germany, 1997.
[22] PWT-PLATON for Windows Taskbar v1.15, University of Glasgow, 2008.
[23] L. Lopes, E.E. Castellano, A.G. Ferreira, C.U. Davanzo, M.J. Clarke, Inorg. Chim. Acta 358 (2005) 2883.
[24] P.E. Pregosin, R.W. Kunz, ^{13}P and ^{13}C NMR of Transition Metal Phosphine Complexes, Springer-Verlag, Berlin, 1979.
[25] (a) P.E. Garrou, Chem. Rev. 81 (1981) 229;
(b) E. Lindner, R. Fawzi, H.A. Mayer, K. Eichele, W. Hiller, Organometallics 11 (1992) 1033.
[26] G. Exarchos, S.D. Robinson, J.W. Steed, Polyhedron 19 (2000) 1511.
[27] J.C. Briggs, C.A. McAuliffe, G. Dyer, J. Chem. Soc., Dalton Trans. (1984) 423.
[28] A.A. Batista, C. Pereira, S.L. Queiroz, L.A.A. de Oliveira, R.H.D. Santos, M.T.D. Gambardella, Polyhedron 16 (1997) 927.
[29] I. Romero, M. Rodríguez, A. Llobet, M. Collomb-Dunand-Sauthier, A. Deronzier, T. Parella, H. Stoeckli-Evans, J. Chem. Soc., Dalton Trans. (2000) 1689.
[30] J. Polam, L. Porter, J. Coord. Chem. 29 (1993) 109.
[31] M. Akita, Y. Takahashi, S. Hikichi, Y. Moro-oka, Inorg. Chem. 40 (2001) 169.
[32] S. Goswami, L.F. Falvello, A. Chakravorty, Inorg. Chem. 26 (1987) 3365.
[33] B. Kukovec, I. Kodrin, Z. Mihalic, K. Furic, Z. Popovic, Inorg. Chim. Acta 363 (2010) 1887.
[34] A.B.P. Lever, Inorg. Chem. 29 (1990) 1271.
[35] M. Al-Noaimi, Polyhedron 29 (2010) 3214.
[36] B.K. Ghosh, A. Chakravorty, Coord. Chem. Rev. 95 (1989) 239.
[37] M.O. Santiago, C.L.D. Filho, I.S. Moreira, R.M. Carlos, S.L. Queiroz, A.A. Batista, Polyhedron 22 (2003) 3205.
[38] L.F. Szczepura, K.J. Takeuchi, Inorg. Chem. 29 (1990) 1772.
[39] A.B.P. Lever, Electronic Absorption Spectroscopy, second ed., Elsevier Publishing Co., Amsterdam, 1985.
[40] (a) R. Crutchley, B. Lever, Inorg. Chem. 21 (1982) 2276;
(b) R.J. Crutchley, K. McCaw, F.L. Lee, E.J. Gabe, Inorg. Chem. 29 (1990) 2576.